



Conventional and advanced imaging throughout the cycle of care of gliomas

Gilles Reuter^{1,2} · Martin Moïse³ · Wolfgang Roll⁴ · Didier Martin¹ · Arnaud Lombard¹ · Félix Scholtes^{1,5} · Walter Stummer⁶ · Eric Suero Molina⁶

Received: 3 August 2020 / Revised: 18 November 2020 / Accepted: 23 November 2020
© Springer-Verlag GmbH Germany, part of Springer Nature 2021, corrected publication 2021

Abstract

Although imaging of gliomas has evolved tremendously over the last decades, published techniques and protocols are not always implemented into clinical practice. Furthermore, most of the published literature focuses on specific timepoints in glioma management. This article reviews the current literature on conventional and advanced imaging techniques and chronologically outlines their practical relevance for the clinical management of gliomas throughout the cycle of care. Relevant articles were located through the Pubmed/Medline database and included in this review. Interpretation of conventional and advanced imaging techniques is crucial along the entire process of glioma care, from diagnosis to follow-up. In addition to the described currently existing techniques, we expect deep learning or machine learning approaches to assist each step of glioma management through tumor segmentation, radiogenomics, prognostication, and characterization of pseudoprogression. Thorough knowledge of the specific performance, possibilities, and limitations of each imaging modality is key for their adequate use in glioma management.

Keywords High-grade gliomas · Glioblastoma · Magnetic resonance Imaging · Diffusion magnetic resonance imaging · Positron emission tomography

Introduction

Before surgery (Table 1)

Is it a glioma?

Magnetic resonance imaging (MRI) is the workhorse of initial workup for intracerebral masses. The minimum standard

protocol includes 3D pre-contrast T1-weighted (3D T1wPre), fluid attenuation inversion recovery (FLAIR), diffusion-weighted imaging (DWI), T2-weighted (T2W), and post-contrast T1-weighted (3DT1wPost) sequences [33].

Conventional imaging of glioma Administration of gadolinium (GD)-based contrast agents reveal blood-brain-barrier disruptions, reflecting tumor infiltration and angiogenesis in glioma. Mainly in high-grade glioma, comparison between pre- and post-contrast T1W images defines the area of central tumor invasion, often associated with (non-enhancing) central necrotic tissue, sometimes hemorrhagic brain tissue and/or central cysts. Cystic components are identified in T2W images through T2-hyperintensity. The classical appearance of glioblastomas (GBM) consists of an area of ring enhancement surrounded by a hypo-T1/hyperT2 zone of brain edema and tumor infiltration. Contrast enhancement is also common in other high-grade gliomas (HGG). Enhancement pattern is associated with tumor aggressiveness [84] and angiogenesis-associated genes [94]. Although common, it is however neither a sufficient nor necessary condition in HGG MRI. About one-third of non-enhancing gliomas are HGG, especially in elderly population [104], and one-third of HGG do not enhance, especially in

✉ Gilles Reuter
gilles.reuter@chuliege.be

¹ Department of Neurosurgery, University Hospital of Liège, Liège, Belgium
² GIGA-CRC In-vivo Imaging Center, ULiege, Liège, Belgium
³ Department of Radiology, University Hospital of Liège, Liège, Belgium
⁴ Department of Nuclear Medicine, University Hospital of Münster, Münster, Germany
⁵ Department of Neuroanatomy, University of Liège, Liège, Belgium
⁶ Department of Neurosurgery, University Hospital of Münster, Münster, Germany

Table 1 Indicative imaging features of glioma: before surgery

<i>MRI Mimics of GBM</i>				
Brain Abscess	Encephalitis	Inflammatory diseases	Cerebral lymphoma	Metastases
Absence of normal peaks in spectroscopy	T2 hyperintensity in the limbic system	Spectroscopy non-discriminant	May or may not enhance	Variable ADC
A typical peaks: acetate, pyruvate, succinate	Rare gadolinium enhancement	High or low ADC	Extensive T2 hyperintensity	Low ADC if mucinous
ADC reduced if purulent	Spectroscopy resemble low-grade glioma	Low rCBV compared with normal brain tissue	Low ADC (high cellularity)	ADC higher than in HGG in peritumoral area
High ADC in abscess walls	Low ADC		Lower rCBV than HGG	Low rCBV in peritumoral area
Reduced rCBV			Signal overshoot (contrast medium leakage)	
<i>Prognosis</i>				
FET-PET interpretation	MGMT promoter methylation	IDH Mutation	1p/19q Codeletion	
Aggressiveness correlated with early peak	Higher ADC if methylated	Single lobe, frontal, cysts, secondary locations, sharp delimitation	May or may not enhance	
May be positive in nonglial tumors (e.g., metastases)	Moderate rather than intense elevation of rCBV elevation if methylated	Large portion of non-enhancing tissue	Fuzzy delimitations	
Higher TBR max in HGG than LGG	Increased K-Trans	Lower rCBV than IDH-wt	Heterogeneous T2	
Low-grade oligodendrogliomas present high ¹⁸ F-FET uptake		Presence of 2-hydroxyglutarate (2-HG)	> 40% calcifications	
			High rCBV and high ¹⁸ F-FET uptake	
<i>Preoperative planning</i>				
Hotspots	Factors influencing functional MRI (fMRI)	Factors influencing diffusion-weighted imaging (DWI)		
High choline/NAA	Proximity with air cells, large cortical veins	Coexistent/coalescent fibers		
High rCBV	Mass effect, edema	Fiber bundle infiltration (diffusivity reduction)		
High ¹⁸ F-FET uptake	Anxiety, pain, attention deficit	Fiber bundle edema (enhanced diffusivity)		
	Elderly population			

isocitrate dehydrogenase (IDH)-mutated tumors [128]. Twenty-six to forty-six percent of low-grade gliomas exhibit some degree of contrast enhancement, especially gangliogliomas, pilocytic or low-grade astrocytomas, and, rarely, low-grade oligodendrogliomas [130].

In MRI, HGG is thus suggested by contrast enhancement (nodular, patchy, or ring-like [128]) with or without central necrosis and intratumoral hemorrhage (both better appreciated on T2*), with or without mass effect, with ill-shaped contour associated with central T2 hyperintensity, central FLAIR hyper- or hypointensity and peritumoral ill-defined FLAIR.

Computerized tomography (CT) can show central, peripheral, or ribbon-like calcifications, suggestive of oligodendroglioma tumors [97]. Due to its accessibility, CT remains important in emergency conditions and in cases of rapid decline where intratumoral hemorrhage is possible [127].

For systematic and reproducible interpretation of glioma imaging features, standardized approaches have been proposed. The Visually Accessible Rembrandt Images (VASARI) feature set is a rule-based lexicon to improve the reproducibility of glioma interpretation. It comprises 25 visual criteria, including tumor location, lesion center laterality, eloquent brain involvement, enhancement quality, proportion enhancing, T1/FLAIR ratio, diffusion characteristics. It has been shown to improve interpretation and reproducibility of glioma description [98]. The meaning of VASARI features have been made explicit via the design and implementation of a specialized ontology, called VASARI ontology [6]. Also, inter-reader variations are being tackled by machine learning and fully-automated segmentation [98].

Advanced imaging studies Diffusion-weighted imaging (DWI) measures random motion of water molecules within

each MRI volume unit (voxel). Water movements can be restricted by high cellularity (tumors), high viscosity (necrotic abscesses), or cytotoxic edema (acute ischemic injury). DWI acquisitions being T2W sequences, it is necessary to withdraw the influence of T2-hyperintensity on DWI signal by calculating the apparent diffusion coefficient (ADC).

Perfusion-weighted imaging (PWI) estimates blood perfusion of the investigated tissue. Multiple acquisitions will detect either an exogenous marker (GD, in dynamic susceptibility contrast (DSC), and dynamic contrast-enhanced (DCE)) or an endogenous marker (Arterial Spin Labelling (ASL)). Parameters that can then be extrapolated include cerebral blood flow (CBF), regional cerebral blood volume (rCBV), and blood-brain barrier permeability.

Magnetic resonance spectroscopy (MRS) analyses parenchymal chemical composition over one or several voxels, where metabolites are quantified at the millimolar scale. N-Acetyl-aspartate (NAA) is a marker of neurons, creatine (Cr) is supposed to be constant in normal and pathological situation and thus acts as internal reference, choline (Cho) is a marker of cell membrane breakdown, myo-inositol (mI) reflects normal glia, lactate (Lac) is a marker of anaerobic metabolism, and free lipids (Lip) are markers of necrosis.

MRI mimics of high-grade gliomas

Infectious disease: brain abscess Brain abscesses are more common in immunocompromised hosts. Pulmonary shunts favor brain abscesses [28]. MRS may show the absence of normal brain peaks (NAA, Cr, Cho) but may show peaks of atypical metabolites: acetate, pyruvate, succinate [44]. ADC is generally markedly reduced in the central portion of the abscess due to pus viscosity, but not necessarily in the walls of the abscess, which may harbor higher ADC values than tumoral cystic walls [23]. rCBV is also frequently reduced compared with necrotic or cystic neoplastic walls [23].

Infectious disease: encephalitis Acute encephalitis may present as T2 hyperintensity in the limbic system that is often asymmetrical or unilateral. Contrast enhancement may rarely be encountered [12]. MRS of encephalitis resembles low-grade gliomas with elevation of the choline peaks and reduction of the NAA peaks. ADC is typically low, especially if the examined brain tissue is infarcted [2].

Inflammatory diseases Acute monophasic syndromes, variants of multiple sclerosis, such as Marburg variant or Balo's concentric sclerosis, may be misdiagnosed as HGG. In the case of a fulminant mass lesion (Fig. 1), spectroscopy cannot formally discriminate between the two, since these lesions may also harbor high choline and low NAA levels. ADC values can be high or low and rCBV is lower than normal brain tissue, which is generally the contrary of high-grade gliomas [22].

Cerebral lymphoma Primary central nervous system lymphoma (PCNSL) is rare, as it comprises only 2% of extranodal lymphomas, but is more frequent in the immunocompromised population. In the setting of rapidly progressive neurological deterioration, lymphoma can masquerade as GBM. Both may or may not enhance, can be surrounded with extensive T2 hyperintensity that respects the cortical ribbon integrity, and have generally low ADC values in the core of the tumor due to their very high cellularity. In immunocompromised patients, lymphoma can harbor a necrotic component as well. The rCBV of these tumors is significantly lower than that of HGG. In PWI lymphomas tend to show a signal overshoot (a signal higher than before perfusion), due to the T1 effect of strong contrast medium leakage into the interstitium [47].

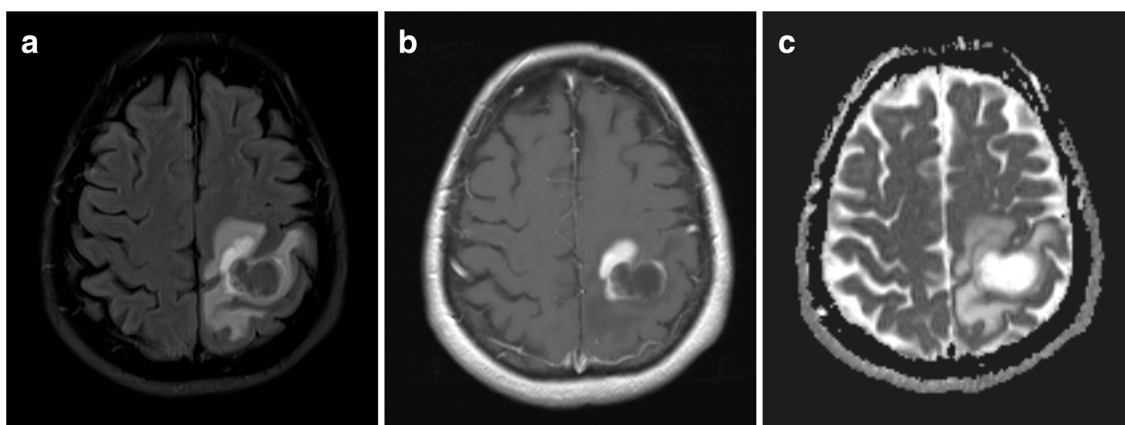
Metastases Metastases can be mistaken for GBM, especially if no primary tumor is found, which is the case despite complete workup in approximately 9% of solitary brain [39]. Small metastases may be detected only on T2/FLAIR, but generally, metastases tend to show (relatively homogeneous pseudo-spheroid) enhancement. A sharp delimitation can in most cases be seen between the metastasis and adjacent brain tissue, but perilesional infiltration can be more prominent in some cases [10]. Peritumoral edema generally respects the cortical ribbon. MRS is not helpful in the discrimination between metastasis and glioma, just as very low central ADC can be found in mucinous metastasis, mimicking brain abscess [93]. ADC values of metastasis are variable and overlap with that of primary neoplasms. However, ADC in the peritumoral area is generally higher in metastasis than in gliomas because of subtler peritumoral cellular infiltration, if there is any. rCBV is elevated in the core of metastases, as in HGG, and perfusion markers overlap [2]. The study of rCBV in the peritumoral zone can efficiently help in differentiating HGG with tumoral infiltration (high rCBV) from metastases with vasogenic edema (low rCBV) [82]. (Fig. 2).

Molecular correlates

Because of the differential response to adjuvant therapy, molecular factors have become crucial in the management of glioma, as evident in the most recent revision of the World Health Organization classification of central nervous system tumors in 2016 [78].

MGMT methylation In GBM, the methylation of O-methylguanine-DNA methyltransferase (MGMT) promoter is associated with a better response to adjuvant therapy with combined alkylating therapy (temozolomide) and radiation therapy. Median survival is 22 months if MGMT promoter methylation is present vs. 15 months if it is absent [48]. It is present in approximately 45% of GBM [48]. The presence of MGMT methylation also provides better outcomes in grade III gliomas (41.6 months of median survival if present vs. 16.9 months if absent [132]) due

Baseline



+ 17 months

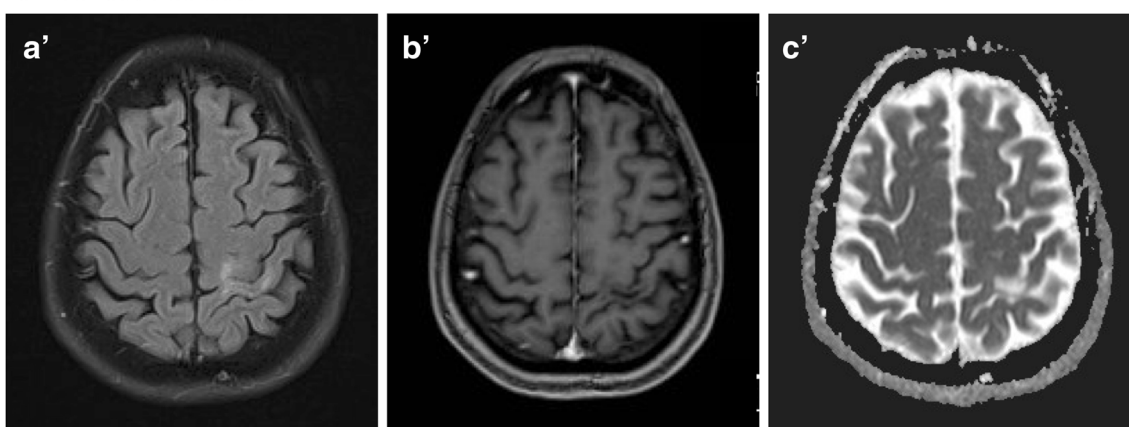


Fig. 1 Tumefactive demyelinating lesion 69-year-old female with history of bilateral optic myelitis, right-side numbness, and paresis. MRI brain scans. A-A') FLAIR. B-B') T1W+C. C-C') ADC cartography. Baseline MRI scan shows a necrotic left parietal lesion (post-central gyrus) with hyper-T2 enhancing compound (incomplete ring enhancement). There is

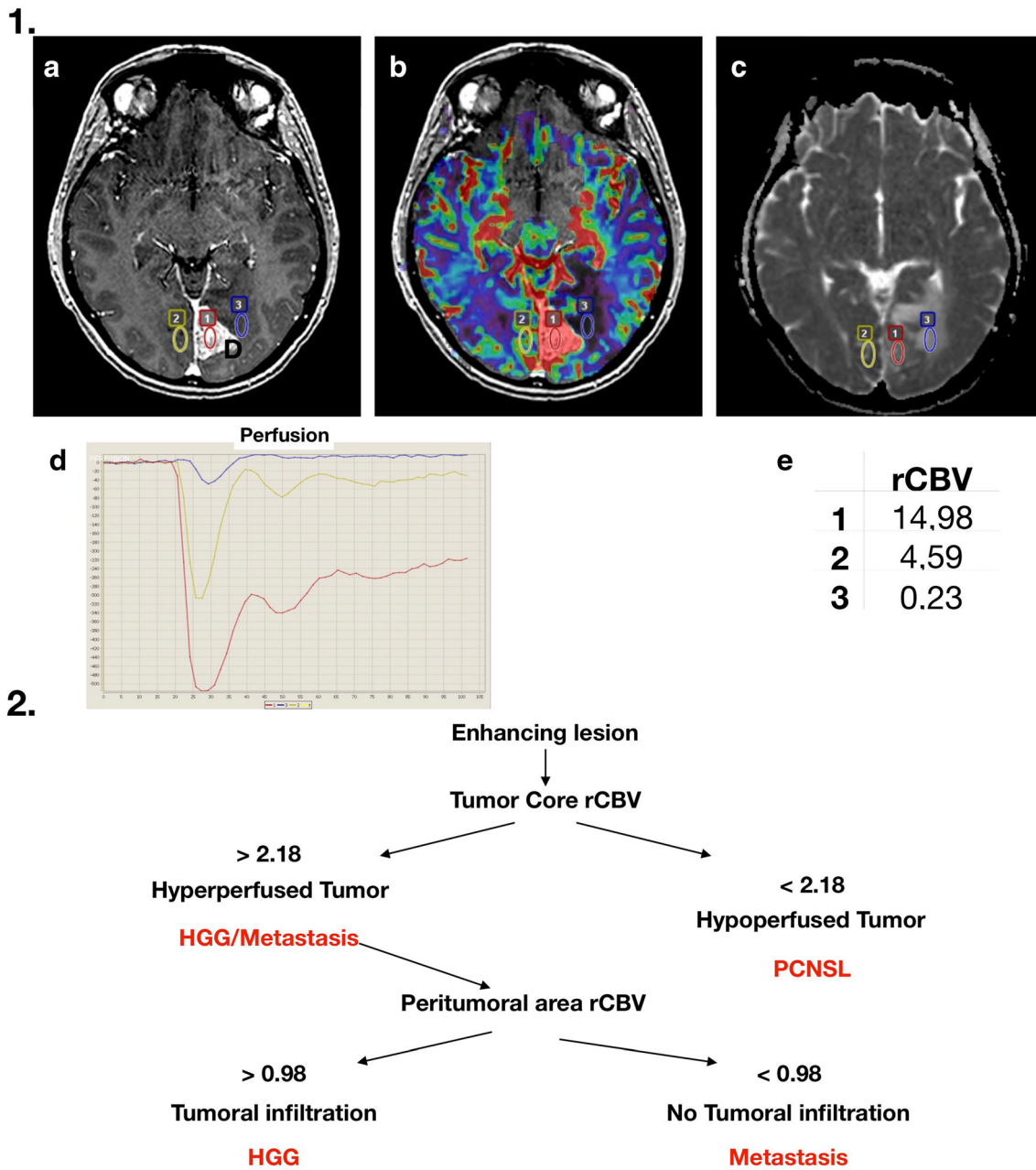
no restriction of diffusion. Patient was treated with plasmapheresis and rituximab IV injections. MRI control 17 months later shows complete resolution of the lesion with glial scar. Those findings are in keeping with neuromyelitis optica spectrum disorder with favorable outcome

to the co-occurrence of IDH mutation and MGMT promoter methylation.

Conventional MRI cannot help predicting MGMT promoter methylation [34]. ADC values tend to be higher in methylated GBM, especially when examined in histogram analyses rather than with standard ADC mapping. Moderately elevated rather than very elevated rCBV is indicative of methylation [108]. A predicting model combining tumor location, necrosis, ADC, and rCBF measured with ASL was able to detect MGMT methylation with 91% sensitivity [46].

IDH mutation IDH mutation is present in the majority of grades II and III glial tumors and is a marker of secondary glioblastoma ($\approx 5\%$ of all glioblastomas). IDH-mutated tumors have a better prognosis than IDH-wild-type (IDH-wt) tumors. The prognosis of lower grade gliomas without IDH mutation is similar to that of GBM.

IDH-mutated tumors tend to be more frequently found in a single lobe, especially the frontal lobe, harbor more cysts, and present with more secondary locations. They often present sharp MRI delimitation and large portions of non-enhancing tissue [21]. rCBV is higher in IDH1-wt GBM than in IDH1 mutant GBM [120]. MR spectroscopy might help to detect IDH-mutated glioma cells which contain high levels of 2-hydroxyglutarate (2HG). This metabolite is normally undetectable, but present at very high concentration (up to 100-fold) in IDH-mutant glioma. Spectroscopy is sensitive and specific for detecting IDH-1 and IDH-2 mutation via 2HG detection [25]. Detection of 2HG is correlated with response to treatment: 2HG levels decline after adjuvant treatment in IDH-mutant glioma [7]. Finally, prediction of IDH-mutation status might be possible using dynamic ^{18}F -fluoroethyl-L-tyrosine positron emission tomography (^{18}F -FET-PET) correlating shorter TTP to more aggressive IDH1-wt glioma [124, 125].



Adapted with permission from Neska-Matuszewska et al. 2018

Fig. 2 Brain metastasis. **1.** 41-year-old female with personal history of HER2-positive breast cancer and occipital headaches. (A) T1W+C. (B) Corrected rCBV fused with T1W+C. (C) ADC mapping. Enhanced parafalcorial left occipital lesion with peritumoral edema and no restricted diffusion. ROI 1 is placed within the lesion and confirm the hypervascularization compared with ROI 2 (contralateral normal brain). ROI 3 indicates hypoperfused perilesional edema, in keeping with the

absence of infiltrative cells. Those findings are in keeping with intra-axial brain metastasis. **2** Diagnosis algorithm of a T1+Gd enhancing lesion using perfusion-weighted MRI (PWI). First, the tumor core is analyzed, if it is highly hypoperfused, primary central nervous system lymphoma (PCNS) is probable, if not, the peritumoral non-enhancing tissue is analyzed. If the perfusion in that area is high, high-grade glioma (HGG) is probable, if not, metastasis is more probable

1p/19q codeletion 1p/19q codeletion is a necessary condition for the diagnosis of oligodendroglioma. Prognosis is better than in glioma without 1p/19q deletion: in a group of patients with grades II and III tumors, patients with 1p/

19q codeletion and IDH-mutation had a median survival of 8.0 years compared with patients without 1p/19q codeletion but with IDH-Mutation who had a median survival of 6.3 years [31]. Patients with 1p/19q codeletion

seem to benefit from procarbazine, lomustine, and vincristine as adjuvant treatment. This is not the case for patients without codeletion.

In oligodendroglioma, contrast enhancement may or may not be present and tumor margins are fairly indistinct. If a sharp border is present, it is more likely a 1p/19q-intact tumor [59]. T2 signal intensity appears more heterogeneous, especially if the mid-frequency domain of the T2 signal is measured with S-transform analysis [19]. Image texture can be defined as the heterogeneity intensity of an image. Quantification of texture was developed for satellite imaging applications and is now applied to the analysis of medical images. An image transform relies on the transform of visual data into frequency description; strong lower frequencies appear as homogeneous smooth regions, whereas strong higher frequencies are seen as heterogeneous detailed regions. The S-transform is a Fourier transform that provides local frequency spectra for each pixel in the image independently and allows a pixel-by-pixel examination of image texture. Calcifications are frequent (> 40%) [108]. Grade II oligodendroglioma often exhibit high rCBV values [58] and relatively high uptake of ^{18}F -FET [124]. Thus, IDH-mutated 1p/19q codeleted tumors are difficult to differentiate from glioblastoma or high-grade astrocytoma with ^{18}F -FET-PET alone [56].

Prognostication Molecular characteristics are directly correlated to tumor aggressiveness. Some tumor properties, such as cellularity, vascularity, and metabolism, can be extrapolated from advanced imaging modalities [32]. Apart from MGMT, IDH, and 1p/19q cited above, it can be useful to detect other molecular markers that correlate with prognosis. Complex imaging features, generally called radiophenotypes, are currently being investigated for almost any predictive and prognostic somatic mutation of glioma. In one investigation, TP53, RB1, NF1, EGFR, and PDGFRA were associated with conventional imaging features such as necrosis, degree of enhancement, and edema [27]. In another study, EGFR amplifications and CDKN2A loss were associated with high rCBV [68]. mTOR-EGFR pathway activation is also associated with high rCBV [76] and tumors with EGFR amplification tend to occur in the left temporal lobe [35]. With more complex multimodal imaging techniques, radiophenotypes can predict key driver mutations in EGFR, PDGFRA, CDKN2A, and RB1 with 75%, 77%, 87.5%, and 87.5% accuracy [50].

PET-imaging with radiolabeled amino acids Positron emission tomography (PET) performed with radiolabeled amino acids, e.g., ^{18}F -FET, has emerged as a useful tool in glioma assessment, allowing for the visualization and quantification of tumor features on a molecular level beyond morphological imaging [73]. Evaluation is usually based on 20–40 min post-injection (p.i.) images. Important parameters are the

maximum tumor-to-brain ratio (TBRmax) and the biological tumor volume (BTv), corresponding to the ^{18}F -FET positive tumor volume after application of a threshold of TBR > 1.6 [116].

TBRmax is higher in high-grade glioma than low-grade diffuse astrocytoma. However, some low-grade tumors, such as oligodendroglioma (IDH-mutated and 1p/19q codeletion), can also show high ^{18}F -FET uptake [51, 124]. Recently, C-Methionine PET/MRI data with machine learning algorithm was able to decipher higher TBR values in grades II and III 1p19q codeleted tumor than in grades II and III non-codeleted tumors [65]. Importantly, some low-grade glioma might be FET negative. Specificity of static ^{18}F -FET-PET to distinguish glioma and other brain lesions is further limited by tracer uptake in nonglial brain tumors (e.g., metastases) and non-neoplastic brain lesions (lower TBR) [51]. Dynamic ^{18}F -FET-PET, where tracer's radioactivity is monitored from the injection up to 40–50 min p.i., offers time-activity curves (TAC) with additional information on tumor grading and mutation status, increasing sensitivity and specificity compared with static ^{18}F -FET-PET. While HGG often show an early peak followed by decreasing TAC, low-grade tumors and non-neoplastic lesions often exhibit slowly increasing TAC [57]. Quantitative parameters derived from dynamic ^{18}F -FET-PET, such as time-to-peak (TTP), might provide additional information for brain tumor assessment and outcome prediction [115].

Perspectives These PET and aforementioned MRI biomarkers that could preoperatively help to predict tumor grading and molecular variants, providing prognostic factors even before histological diagnosis, are still under investigation. The combination of state-of-the-art MRI and PET in increasingly available hybrid PET-MR-systems offers new opportunities for comparative studies extracting differential morphological and molecular tumor features. For the direct comparison of different advanced MRI parameters and amino acid PET, we refer to a recent review by Lohmann et al. [77].

Radiomics Radiomics, or quantitative radiographic phenotyping (www.radiomics.io), is a translational field of biomedical research aiming to obtain molecular patterns through different imaging modalities. Although it offers promising perspectives for clinical decision-making and targeted treatment, there are still challenges to overcome [99]. In addition, artificial intelligence approaches as deep learning [105], neural networks, and convolutional neural networks are being developed. The aim is to help, if not replace, the clinician in grading prediction, genetic information, preoperative planning, intraoperative treatment planning, histopathologic diagnosis, radiation, post-treatment follow-up, and outcome prediction [109]. Even if surgery remains the mainstay in the initiation of glioma treatment in the majority of cases for low- [55] and high-

grade tumors [112], in some patients, e.g., in poor clinical conditions, MRI techniques approaching the diagnostic yield of histology could avoid any type of surgery, including purely diagnostic needle biopsy.

Not confined to MRI techniques, machine learning and artificial intelligence techniques are also investigated for PET imaging alone for survival prediction [89], tumor segmentation [16], pseudoprogression [64], or in combination with MR for molecular subtyping [65, 79] and survival prediction [91].

Extent of the tumor

Preoperative planning The intratumoral histological heterogeneity of glioma is a possible reason for treatment failure [121]. Commonly, the most malignant portion that has been subjected to histology will define grading.

In a stereotactic biopsy series, PWI could identify high cancer burden areas (hotspots), especially in non-enhancing tumors [66]. ^{18}F -FET-PET can identify anaplastic foci in low-grade glioma [70, 110]. In GBM, MRS can also help identify hotspots, where choline to NAA levels are correlated to cell density in the contrast-enhancing region and in the T2w abnormality as well as in tissue outside both abnormalities [29].

The extent of GBM resection directly correlates with survival [112]. Complete removal of enhancing tumor (CRET) with some peritumoral FLAIR abnormality, when feasible, may improve overall survival compared with resection of enhancing tissue only. Provided that no new neurological deficit occurred during surgery, median survival time was 20.7 months at or over a cut-off of 53.21% of total FLAIR abnormality resection vs. 15.5 months under 53.21% [75, 96].

Lower grade glioma can be identified as areas of hypertintensity in T2-weighted and FLAIR images, with different degrees of heterogeneity and hypointensity on T1-weighted images. As stated above, contrast enhancement is not exceptional in lower grade glioma. Maximal resection of diffuse low-grade glioma according to functional (not only anatomical) boundaries is associated with increased overall survival. The surgical goal should therefore be to remove the entire T2/FLAIR abnormality *if function can be preserved*. If resection of more than 90% of tumor volume can be achieved, 97% of patients will survive more than 5 years [107]. Especially in IDH-mutated astrocytomas, gross total resection is associated with better prognosis, as even small residual tumor negatively affects overall survival [62, 133]. For lower grade gliomas situated near eloquent brain regions, subtotal resection preserving the eloquent region can still lead to better survival [52]. Awake craniotomy with electrical mapping, tractography, functional MRI, and intraoperative MRI are increasingly used in order to maximize extent of resection.

Detecting function Functional MRI (fMRI) is based on local variations in oxygen demand in connection with neuronal activation. fMRI may delineate functional brain areas sufficiently to influence surgical approaches and evaluate the probability of postoperative deficits.

Beyond the approximate nature of the detection of functional areas, fMRI presents other limitations. The tumor itself can induce cerebral reorganization and false positive and negative results [106]. fMRI signal is not reliable in the inferior temporal lobe or in the orbito-frontal cortex, close to air cells. Large cortical veins can distort fMRI signal [4]. HGG mass effect and edema can induce brain warping and decrease or abolish fMRI signal [38, 69]. Anxiety, pain, and attention deficits influence the participation to the task and fMRI is highly sensitive to motion artifacts [106]. fMRI signal decreases with age so old patients must be analyzed cautiously.

Diffusion-weighted images and tractography Tractography, the reconstruction of white matter bundles, is based on DWI. It may preoperatively indicate the approximate location of eloquent white matter tracts.

Again, this technique presents limitations. Without going into detail, voxels will be given a single fiber orientation. If fibers coexist, cross or coalesce, the algorithm leading to the reconstruction of the tract may lead to false negative images, i.e., the reconstructed fiber orientation not following an existing path (tract). If cellular infiltration is present, the diffusion will be more restricted and the tract might not be detected. Fiber bundles carrying neurological function may thus not be seen in tractography. Inversely, edema can lead to artificially elevated diffusion and thus can lead to false positives, i.e., the fiber reconstruction following a non-existing path.

^{18}F -Fluoroethyl-L-tyrosine positron emission tomography

Preoperative ^{18}F -FET-PET has been shown to depict anaplastic foci, which can be found in 44–55% of low-grade glioma [70, 110]. These regions can be specifically targeted during surgery to ensure precise sampling of the tumor, leading to accurate grading. Furthermore, in HGG, tracer uptake in ^{18}F -FET-PET can depict larger tumor regions compared with conventional GD-enhanced MRI [20]. Using the tumor volume depicted by both amino acids ^{18}F -FET and ^{11}C -methionine (MET), Pirotte and colleagues demonstrated that complete resection of this area leads to significantly longer overall survival in HGG patients [92].

During surgery (Table 2)

Surgical adjuncts

The extent of resection is an essential surgical outcome that influences the rate of recurrence, as well as progression-free and overall survival [71, 101, 111]. To date, in high-grade

Table 2 Indicative imaging features of glioma: during surgery

Neuronavigation	Ultrasound	5-ALA	Intraoperative MRI (iMRI)	Raman spectroscopy
Useful for craniotomy planning	Inexpensive	Real-time 2D information without brain shift limitation.	Allows resection monitoring	Reliable tissue diagnosis in the operating room
Limited by brain shift	Not limited by brain shift	Tumor depiction beyond MRI borders Limited by: blood, overhanging edges, photosensitization	Expensive and increases surgery time	

glioma, gross total resection is defined as CRET and remains the goal of malignant glioma surgery. However, tumor margins are difficult to define during surgery. Hence, various surgical adjuncts have been introduced over the past decades. Neuronavigation, fluorescence-guidance, intraoperative MRI (iMRI), and ultrasound are established surgical tools in neurosurgical practice [49].

Neuronavigation represented the first step in increasing intraoperative imaging in the surgical flow. However, this tool suffers from potential inaccuracy due to brain shift and interrupts surgery for reorientation [85, 134]. It is used to tailor craniotomies and provide orientation during surgery. Ultrasound is an inexpensive and rapid way of monitoring resection (without the disadvantage of brain shift).

Fluorescence-guidance with 5-aminolevulinic acid (5-ALA), provides real-time information within the operating surgical field without concern for brain shift. It is approved for use in Europe, USA, and numerous other countries. One drawback of fluorescence guidance is that it only provides 2-dimensional information. Also, fluorophores can be obscured by blood, hiding important tumor tissue [113]. 5-ALA is given orally 4 h prior to induction of anesthesia at a dose of 20 mg/kg b.w. Fluorescence maximum in tumor tissue will be found 7–8 h after administration of 5-ALA [61]. CRET has been to date reported to be up to 96% when utilizing fluorescence-guidance with 5-ALA in a contemporary neurosurgical facility [103]. Another fluorescent agent, fluorescein, gained popularity over the last years after the introduction of a novel filter (YELLOW 560, Zeiss, Oberkochen, Germany) that provides superior background illumination compared with the 5-ALA filter system (BLUE 400, Zeiss, Oberkochen Germany) [102]. Fluorescein marks areas of blood-brain barrier breakdown and is to date still off-label. Disadvantages are unspecific propagation into the edema zone or into the surgical cavity during resection. Furthermore, time dependency is not well studied for this fluorophore, hampering its visualization during surgery [118, 119]. In low-grade glioma, 5-ALA-mediated fluorescence-guidance can indicate anaplastic foci providing accurate grading [53].

Albeit expensive, iMRI has also shown it might increase the extent of resection. Thus, potentially, it can be used to monitor resection of non-enhancing, non-fluorescing low-

grade glioma tissue [117]. This 3-dimensional tool locates residual tumor tissue in deep brain tissue. High costs and an increase in surgery time are potential drawbacks.

Another adjunct that merits mention is Raman spectroscopy. This surgical adjunct is a label-free optical imaging of fresh surgical specimens with potential for ex vivo and in vivo implementation, adding the advantages of computer-aided diagnosis and machine learning for tissue diagnosis [49]. It provides reliable tissue diagnosis within the operating room, potentially replacing fresh frozen sections in the future.

After surgery (Table 3)

Postoperative imaging

Postoperative MRI shows the extent of resection. If residual tissue is present, second-look surgery for GBM can be an option, as incomplete resection carries almost the same overall survival rates than biopsy alone [67, 88]. Postoperative MRI should be performed within 48 h of surgery since early sub-acute blood will appear hyperintense in native T1W pre-contrast images. As soon as 17 h after surgery, a linear reactive non-tumoral enhancement may occur and significantly increases after 45 h post-surgery [14].

In a prospective exploratory observation analysis, size of residual ¹⁸F-FET-PET active tumor tissue was likewise correlated with poorer outcome [81]. The authors demonstrated that even in those patients with CRET in MRI, postoperative residual ¹⁸F-FET-PET volume > 4.3 cm³ was a critical cut-off to predict worse overall survival.

Systematic postoperative CT is not routinely recommended as it is unlikely to modify management if postoperative neurological examination is unchanged. Nonreliable examinations or worrisome clinical changes must lead to early postoperative CT [5, 37].

Complications

The incidence of documented complications after malignant brain tumor surgery has been evaluated at 3.4% [30]. New or worsened neurological deficits significantly reduce quality of

Table 3 Indicative imaging features of glioma: after surgery

Postoperative imaging		Complications	
Linear enhancement will appear early (17 h post-surgery)		Ischemia: 31% in first surgery; 80% in recurrent glioma, total volume of infarcted tissue correlated with new deficits and inversely to OS	
CRET with FLAIR resection (> 53.21% of FLAIR abnormality): OS 20.7 months vs. 15.5 months, provided that no new neurological deficit occurred		Hematomas are rarely symptomatic (1%)	
Better prognosis if < 4.3 cm ³ of residual FET uptake		Surgical site infection: higher risk for GBM in the elderly population, ADC not as discriminatory as in primary brain abscess during the postoperative phase (3 months)	
<i>Radiation therapy planning</i>			
Conventional planning	Advanced	FET-PET	
Surgical cavity+ any residual enhancing tumor (GTV) + 2-3 cm margin (CTV) + 3-5 mm (PTV)	DWI can indicate the type of recurrence	Incorporation of FET-PET in the planning process leads to field reduction	
80–90% of recurrences will be located in the field	High choline/Naa and high rCBV areas can be included in the planning		
Cognitive side effects dose related	High infarcted volume is associated with multifocal progression		
<i>Response to treatment</i>			
RANO criteria	Progression vs. Pseudoprogression	Antiangiogenic Therapy	Immunotherapy
A FLAIR increase on a stable/increasing dose of steroids is also compatible with progression	Up to 36% of pseudoprogression in GBM, pseudoprogression and true progression can coexist	No effect on overall survival	iRANO: control MRI at 3 months in cas of new enhancement
Limitation: measured on the maximal diameters of the tumors and HGG grow in an irregular pattern	Monitoring rCBV: progressive elevation suggests true progression, stable or declining rCBV suggests pseudoprogression	Associated with diffusion restriction and T1 hyperintensity in periventricular zone	
	Lower rCBV (<2 ml/100 g) and MAX rCBV (<2.6 ml/100 g) in pseudoprogression		
	FET-PET: low TBRmax and long TTP suggest pseudoprogression		

life and overall survival [96]. It may be caused by incidental resection of functional brain tissue, especially if no intraoperative adjunct is used to localize function [100] and can be intercepted through conventional MRI. Postoperative brain ischemia is found in 31% of newly diagnosed glioma and in 80% of recurrent glioma [43]. They may be clinically silent or have a high impact on autonomy. The total volume of infarcted brain tissue, in DWI, is positively correlated to new neurological deficits [54] and inversely correlated to overall survival, but not to progression-free survival [15].

Slight bleeding in the surgical cavity is frequent, but symptomatic hematoma is rare (approx. 1%) [30].

The incidence of surgical site infection after clean craniotomy is low (1.5%) [122]. It may be higher in the older population with GBM (9.8%) [24] and it does not modify survival rates. Because of postoperative artifacts, ADC is not as discriminatory in postoperative infections as in primary abscesses, where central ADC is generally low; this is not seen in all post-craniotomy infections [11]. Three months after surgery, DWI might regain its validity but the majority of

postoperative infections occur within the first month after craniotomy [11].

Follow-up

Radiotherapy planning

Target volume is based on conventional MRI, including T1+Gd and FLAIR sequences performed at a maximum of 2 weeks before RT. The gross tumor volume (GTV) calculation is based on the surgical cavity + any residual enhancing tumor + a 2- to 3-cm margin for the clinical target volume (CTV) + a 3- to 5-mm margin to account for setup error in the planning of the target volume (PTV) [86]. Smaller CTVs have been tested with similar to better outcomes regarding overall survival [90].

Despite correct planning, most recurrences (80 to 90%) occur in the irradiation field. In addition, some cognitive side effects of radiation are attributed to irradiation of functional brain tissue and tend to be dose-dependent [45, 74]. Therefore, better delineation of the tumor is desirable. The following

tools show promise and may also help in designing clinical trials:

Advanced imaging studies of the invasive tumoral burden

Some diffusion parameters (p for isotropic and q for anisotropic components) may distinguish three different recurrence patterns: a diffuse pattern ($p > q$), a localized recurrence pattern ($p > q$ in one direction), and a limited recurrence pattern ($p \approx q$). Incorporating these data in clinical practice has been proven to reduce the size of the CTV [9].

Furthermore, in the infiltrative portion of GBM, rCBV is elevated, compared with normal-appearing white matter and so is the Choline/NAA ratio [29, 95].

¹⁸F-FET-PET FET-PET might improve the delineation of the target volume by directly detecting metabolically active tumor tissue. CTV margins in glioblastoma patients could be reduced through combined ¹⁸F-FET-PET-MR delineation, compared with MRI alone, without negative impact on the pattern of recurrence [36, 80].

Diffusion and recurrence The total amount of postoperatively infarcted tissue on postoperative diffusion maps is correlated to the type of progression: the highest infarcted volume was correlated with multifocal progression and recurrence with contact to the ventricle or the dura [13].

Response to treatment

The evaluation of response to treatment is defined by the Response Assessment in Neuro-Oncology (RANO) criteria [129], i.e., MRI findings, clinical findings, and the need for corticosteroids. MRI findings include size of enhancing tumor and hyperintense FLAIR regions. Some tumors only progress on FLAIR images, but do not specifically enhance during progression. Therefore, any significant increase of FLAIR hypersignal of a non-enhancing lesion on a stable or increasing dose of corticosteroids meets the criteria for progression. RANO criteria are based on 2-dimensional measurements, the products of the two maximum diameters of the enhancing or FLAIR tissue. This approach is simple. However, many HGG grow in an irregular pattern. In order to obtain a more accurate assessment of tumor size and growth, quantifying the entire tumor with automated computer-assisted volumetric tools can provide more precise measurements [26].

Progression vs. pseudoprogression

Pseudoprogression is defined by the development of new or enlarging enhancement that mimics true progression. In pseudoprogression, the enhancement area will decrease over time contrary to true progression. Pseudoprogression is mostly

encountered after radiotherapy combined with temozolomide for GBM. It may occur as frequently as in 36% of cases [1], typically within the first 3 months after initiation of radiotherapy, but late pseudoprogression can occur up to 18 months after the initiation of radiotherapy [63, 114, 131]. In rare cases, especially with IDH-1 mutation in young patients, contrast-enhancing spots can be considered late-onset pseudoprogression up to a median of 30 months after irradiation [126]. On conventional MRI, it appears as a thick enhancement around the surgical cavity and is virtually inseparable from true progression with this imaging modality alone. In one study rCBV tends to be higher in true progression compared with pseudoprogression with a threshold of 2.0 mL/100 g with high sensibility and sensitivity [72]. Another study has indicated that maximum rCBV was better than rCBV at differentiating true progression from treatment effect when maximum rCBV was set at 2.6 ml/100 g [17]. Nevertheless, pseudoprogression and true progression often coexist. A single MRI session may not help differentiate both entities. Monitoring the rCBV can be needed during the follow-up period, as a linear elevation is associated with progression; stabilization or regression of rCBV is more compatible with pseudoprogression [18]. Adding DTI, ASL, and spectroscopy might improve the accuracy of MRI diagnosis in such instances [123]. PET imaging utilizing the radiolabeled amino acid ¹⁸F-FET has been advocated to distinguish pseudo from real progression [41] as recently emphasized by the PET-RANO group. Besides TBRmax, the evaluation of dynamic FET parameters (TTP) enables differentiation of tumor recurrence from treatment-related changes [3, 42]. (Fig. 3.)

Antiangiogenic therapy

Bevacizumab has no effect on overall survival and its effect on progression-free survival, measured on enhancement, is related to the effect on the blood-brain barrier [60]. The bevacizumab-induced suppression of enhancement was called “pseudoresponse,” and was a driver of the need for MRI protocols accounting for the non-enhancing part of glioma.

Therefore, perfusion imaging studies helped in differentiating non-enhancing tumor from radiation-induced gliosis and edema. Perfusion markers tended to be elevated in the infiltrative part of the tumor [8]. Bevacizumab is also associated with a pattern of persistent restriction of diffusion that may mimic viable tumor, especially in periventricular area and hyperintensity in T1W images, so careful interpretation of diffusion is needed in the context of antiangiogenic therapy [83]. As FET uptake seems partly independent of blood-brain barrier permeability, FET might be useful for longitudinal imaging of patients receiving antiangiogenic therapy [40].

1.

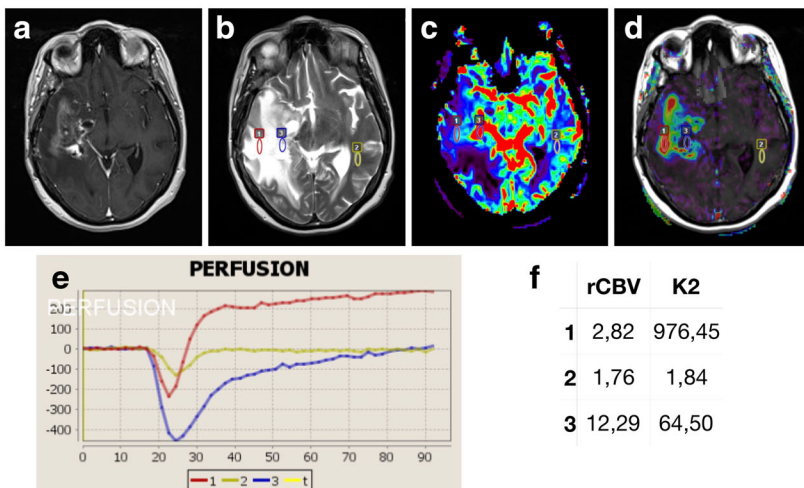
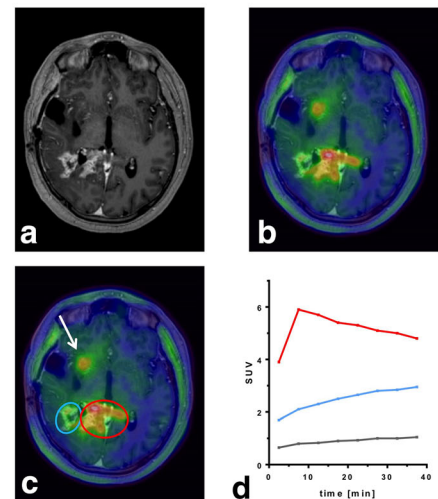


Fig. 3 Coexistent recurrence and pseudoprogression: 1. 48-year-old female, 1-year follow-up after right temporal GBM surgery. MRI brain scan with PWI sequences. (A) T1W+C: multiple ill-defined contrast intakes extending from temporal resection site. (B) T2W showing a large right temporo-parietal hypersignal. (C) Corrected rCBV mapping. (D) DWI K2 (permeability) mapping fused with T1W. (E) rCBV curves. (F) Quantification of rCBV and K2 for each region of interest (ROI). ROI 1 shows no significant rCBV increase (2.82 vs. 1.76 in normal contralateral WM) but major BBB permeability increase: these findings are in keeping with increased permeability such as in pseudoprogression. ROI 3 shows major rCBV (12.29 vs. 1.76 in normal contralateral WM) in keeping with local recurrence. 2. MR (A) and fused PET-MR images

2.



(B) of a patient with a history of anaplastic astrocytoma (WHO grade III) after surgical resection, irradiation, and chemotherapy (temozolomide). Dynamic FET-PET helps to distinguish between irradiation-induced necrosis (blue circle, (C)) with an increasing time activity curve (TAC, (D)) over time (40 min) and progressive tumor tissue (red) with decreasing TAC after an early peak (< 10 min). Both lesions presenting with blood-brain barrier breakdown and leakage of contrast agent in MRI (A). Corresponding TAC of the reference region in the contralateral hemisphere is shown in gray (D). Moreover, a new and small lesion anterior to the resection defect can be easily detected in fused FET-PET-MR (arrow, (C)), with corresponding slight contrast enhancement in MRI (A)

Immunotherapy

There is very little information regarding the treatment-related PET and MRI modifications after immunotherapy. On the basis of RANO criteria [129], the “immunotherapy response assessment in neuro-oncology” (iRANO) was designed in order to address the challenges associated with immune therapy in brain tumors. It is therefore recommended, after any MRI that would show any enhancement increase, to consider the possibility of immunotherapy pseudoprogression and to perform an MRI confirmation 3 months later [87].

Conclusions

Treating patients with glioma requires thorough knowledge of conventional imaging techniques that are of primary importance in every step of their management. Among current advanced imaging techniques, some will be considered conventional in the near future as evidence of their usefulness accumulates. This overview, intended for clinicians, summarizes the state-of-the-art conventional and advanced imaging techniques of glioma management.

Acknowledgments The authors are very grateful to the patients of the CHU of Liège, where the illustrative figures were extracted. We wish to thank Dr. Emilie Lommers and Pr Pierre Maquet for their kind review.

Code availability Not applicable.

Authors' contributions Gilles Reuter had the idea for the article, performed the first literature search, and drafted the work. Eric Suero Molina, Wolfgang Roll, and Martin Moïse critically revised and augmented this review with illustrations. Arnaud Lombard, Felix Scholtes, Didier Martin, and Walter Stummer complemented and nuanced the contents. All authors read and approved the final manuscript.

Data availability Not applicable.

Compliance with ethical standards

Ethical statement Not applicable.

Conflict of interest The authors declare that they have no conflict of interest.

Ethical approval Ethical approval was obtained from the local ethics committee of the University of Liège (B707201316912). All the images we displayed were performed in routine care.

Informed consent We only display MRI and PET-CT brain scans where no identifying information can be found.

Consent to participate No active participation from patients was required for this review.

Consent for publication As every image is fully anonymized and untraceable, the identification risk is virtually absent. The local ethics committee did not require consent for publication.

References

- Abbasi AW, Westerlaan HE, Holtman GA, Aden KM, van Laar PJ, van der Hooft A (2018) Incidence of tumour progression and pseudoprogression in high-grade gliomas: a systematic review and meta-analysis. *Clin Neuroradiol* 28:401–411. <https://doi.org/10.1007/s00062-017-0584-x>
- Al-Okaili RN, Krejza J, Wang S, Woo JH, Melhem ER (2006) Advanced MR imaging techniques in the diagnosis of intraaxial brain tumors in adults. *Radiographics* 26(Suppl 1):S173–S189. <https://doi.org/10.1148/rg.26si065513>
- Albert NL, Weller M, Suchorska B, Galldikis N, Soffiotti R, Kim MM, la Fougere C, Pope W, Law I, Arbizu J, Chamberlain MC, Vogelbaum M, Ellingson BM, Tonn JC (2016) Response Assessment in Neuro-Oncology working group and European Association for Neuro-Oncology recommendations for the clinical use of PET imaging in gliomas. *Neuro-Oncology* 18:1199–1208. <https://doi.org/10.1093/neuonc/now058>
- Alkadhi H, Kollias SS, Crelier GR, Golay X, Hepp-Reymond MC, Valavanis A (2000) Plasticity of the human motor cortex in patients with arteriovenous malformations: a functional MR imaging study. *AJNR Am J Neuroradiol* 21:1423–1433
- Alkhalili K, Zenonos G, Tataryn Z, Amankulor N, Engh J (2018) The utility of early postoperative head computed tomography in brain tumor surgery: a retrospective analysis of 755 cases. *World Neurosurg* 111:e206–e212. <https://doi.org/10.1016/j.wneu.2017.12.038>
- Amdouni EG, B. (2018) Semantic representation of neuroimaging observations: proof of concept based on the VASARI terminology. Paper presented at the International Conference on Knowledge Engineering and Ontology Development, Seville, Spain.
- Andronesi OC, Loebel F, Bogner W, Marjanska M, Vander Heiden MG, Iafrate AJ, Dietrich J, Batchelor TT, Gerstner ER, Kaelin WG, Chi AS, Rosen BR, Cahill DP (2016) Treatment response assessment in IDH-mutant glioma patients by noninvasive 3D functional spectroscopic mapping of 2-hydroxyglutarate. *Clin Cancer Res* 22:1632–1641. <https://doi.org/10.1158/1078-0432.CCR-15-0656>
- Artzi M, Blumenthal DT, Bokstein F, Nadav G, Liberman G, Aizenstein O, Ben Bashat D (2015) Classification of tumor area using combined DCE and DSC MRI in patients with glioblastoma. *J Neuro-Oncol* 121:349–357. <https://doi.org/10.1007/s11060-014-1639-3>
- Berberat J, McNamara J, Remonda L, Bodis S, Rogers S (2014) Diffusion tensor imaging for target volume definition in glioblastoma multiforme. *Strahlenther Onkol* 190:939–943. <https://doi.org/10.1007/s00066-014-0676-3>
- Berghoff AS, Rajky O, Winkler F, Bartsch R, Furtner J, Hainfellner JA, Goodman SL, Weller M, Schittenhelm J, Preusser M (2013) Invasion patterns in brain metastases of solid cancers. *Neuro-Oncology* 15:1664–1672. <https://doi.org/10.1093/neuonc/not112>
- Berndt M, Lange N, Ryang YM, Meyer B, Zimmer C, Hapfelmeier A, Wantia N, Gempt J, Lummel N (2018) Value of diffusion-weighted Imaging in the diagnosis of postoperative intracranial infections. *World Neurosurg* 118:e245–e253. <https://doi.org/10.1016/j.wneu.2018.06.167>
- Bertrand A, Leclercq D, Martinez-Almoyra L, Girard N, Stahl JP, De-Broucker T (2017) MR imaging of adult acute infectious encephalitis. *Med Mal Infect* 47:195–205. <https://doi.org/10.1016/j.medmal.2017.01.002>
- Bette S, Barz M, Huber T, Straube C, Schmidt-Graf F, Combs SE, Delbridge C, Gerhardt J, Zimmer C, Meyer B, Kirschke JS, Boeckh-Behrens T, Wiestler B, Gempt J (2018) Retrospective analysis of radiological recurrence patterns in glioblastoma, their prognostic value and association to postoperative infarct volume. *Sci Rep* 8:4561. <https://doi.org/10.1038/s41598-018-22697-9>
- Bette S, Gempt J, Huber T, Boeckh-Behrens T, Ringel F, Meyer B, Zimmer C, Kirschke JS (2016) Patterns and time dependence of unspecific enhancement in postoperative magnetic resonance Imaging after glioblastoma resection. *World Neurosurg* 90:440–447. <https://doi.org/10.1016/j.wneu.2016.03.031>
- Bette S, Wiestler B, Kaesmacher J, Huber T, Gerhardt J, Barz M, Delbridge C, Ryang YM, Ringel F, Zimmer C, Meyer B, Boeckh-Behrens T, Kirschke JS, Gempt J (2016) Infarct volume after glioblastoma surgery as an independent prognostic factor. *Oncotarget* 7:61945–61954. Doi:<https://doi.org/10.18632/oncotarget.11482>
- Blanc-Durand P, Van Der Gucht A, Schaefer N, Itti E, Prior JO (2018) Automatic lesion detection and segmentation of 18F-FET PET in gliomas: a full 3D U-Net convolutional neural network study. *PLoS One* 13:e0195798. <https://doi.org/10.1371/journal.pone.0195798>
- Blasel S, Zagorcic A, Jurcoane A, Bahr O, Wagner M, Harter PN, Hattingen E (2016) Perfusion MRI in the evaluation of suspected glioblastoma recurrence. *J Neuroimaging* 26:116–123. <https://doi.org/10.1111/jon.12247>
- Boxerman JL, Ellingson BM, Jeyapalan S, Elinzano H, Harris RJ, Rogg JM, Pope WB, Safran H (2017) Longitudinal DSC-MRI for distinguishing tumor recurrence from pseudoprogression in patients with a high-grade glioma. *Am J Clin Oncol* 40:228–234. <https://doi.org/10.1097/COC.000000000000156>
- Brown R, Zlatescu M, Sijben A, Roldan G, Easaw J, Forsyth P, Parney I, Sevick R, Yan E, Demetrick D, Schiff D, Caimcross G, Mitchell R (2008) The use of magnetic resonance imaging to noninvasively detect genetic signatures in oligodendroglioma. *Clin Cancer Res* 14:2357–2362. <https://doi.org/10.1158/1078-0432.CCR-07-1964>
- Buchmann N, Klasner B, Gempt J, Bauer JS, Pyka T, Delbridge C, Meyer B, Krause BJ, Ringel F (2016) (18)F-Fluoroethyl-l-tyrosine positron emission tomography to delineate tumor residuals after glioblastoma resection: a comparison with standard postoperative magnetic resonance imaging. *World Neurosurg* 89:420–426. <https://doi.org/10.1016/j.wneu.2016.02.032>
- Carrillo JA, Lai A, Nghiemphu PL, Kim HJ, Phillips HS, Kharbanda S, Moftakhar P, Lalaeezari S, Yong W, Ellingson BM, Cloughesy TF, Pope WB (2012) Relationship between tumor enhancement, edema, IDH1 mutational status, MGMT promoter methylation, and survival in glioblastoma. *AJNR Am J Neuroradiol* 33:1349–1355. <https://doi.org/10.3174/ajnr.A2950>
- Cha S, Knopp EA, Johnson G, Wetzel SG, Litt AW, Zagzag D (2002) Intracranial mass lesions: dynamic contrast-enhanced susceptibility-weighted echo-planar perfusion MR imaging. *Radiology* 223:11–29. <https://doi.org/10.1148/radiol.2231010594>
- Chan JH, Tsui EY, Chau LF, Chow KY, Chan MS, Yuen MK, Chan TL, Cheng WK, Wong KP (2002) Discrimination of an infected brain tumor from a cerebral abscess by combined MR perfusion and diffusion imaging. *Comput Med Imaging Graph* 26:19–23. [https://doi.org/10.1016/s0895-6111\(01\)00023-4](https://doi.org/10.1016/s0895-6111(01)00023-4)
- Chen YR, Ugiliweneza B, Burton E, Woo SY, Boakye M, Skirboll S (2017) The effect of postoperative infection on survival

- in patients with glioblastoma. *J Neurosurg* 127:807–811. <https://doi.org/10.3171/2016.8.JNS16836>
25. Choi C, Ganji SK, DeBerardinis RJ, Hatanpaa KJ, Rakheja D, Kovacs Z, Yang XL, Mashimo T, Raisanen JM, Marin-Valencia I, Pascual JM, Madden CJ, Mickey BE, Malloy CR, Bachoo RM, Maher EA (2012) 2-hydroxyglutarate detection by magnetic resonance spectroscopy in IDH-mutated patients with gliomas. *Nat Med* 18:624–629. <https://doi.org/10.1038/nm.2682>
 26. Chow DS, Qi J, Guo X, Miloushev VZ, Iwamoto FM, Bruce JN, Lassman AB, Schwartz LH, Lignelli A, Zhao B, Filippi CG (2014) Semiautomated volumetric measurement on postcontrast MR imaging for analysis of recurrent and residual disease in glioblastoma multiforme. *AJNR Am J Neuroradiol* 35:498–503. <https://doi.org/10.3174/ajnr.A3724>
 27. Colen R, Foster I, Gatenby R, Giger ME, Gillies R, Gutman D, Heller M, Jain R, Madabhushi A, Madhavan S, Napel S, Rao A, Saltz J, Tatum J, Verhaak R, Whitman G (2014) NCI workshop report: clinical and computational requirements for correlating imaging phenotypes with genomics signatures. *Transl Oncol* 7:556–569. <https://doi.org/10.1016/j.tranon.2014.07.007>
 28. Comi AM (2011) Presentation, diagnosis, pathophysiology, and treatment of the neurological features of Sturge-Weber syndrome. *Neurologist* 17:179–184. <https://doi.org/10.1097/NRL.0b013e318220c5b6>
 29. Cordova JS, Shu HK, Liang Z, Gurbani SS, Cooper LA, Holder CA, Olson JJ, Kairdolf B, Schreiber E, Neill SG, Hadjipanayis CG, Shim H (2016) Whole-brain spectroscopic MRI biomarkers identify infiltrating margins in glioblastoma patients. *Neuro-Oncology* 18:1180–1189. <https://doi.org/10.1093/neuonc/nov036>
 30. De la Garza-Ramos R, Kerezoudis P, Tamargo RJ, Brem H, Huang J, Bydon M (2016) Surgical complications following malignant brain tumor surgery: an analysis of 2002–2011 data. *Clin Neurol Neurosurg* 140:6–10. <https://doi.org/10.1016/j.clineuro.2015.11.005>
 31. Eckel-Passow JE, Lachance DH, Molinaro AM, Walsh KM, Decker PA, Sicotte H, Pekmezci M, Rice T, Kosel ML, Smimov IV, Sarkar G, Caron AA, Kollmeyer TM, Praska CE, Chada AR, Halder C, Hansen HM, McCoy LS, Bracci PM, Marshall R, Zheng S, Reis GF, Pico AR, O'Neill BP, Buckner JC, Giannini C, Huse JT, Perry A, Tihan T, Berger MS, Chang SM, Prados MD, Wiemels J, Wiencke JK, Wrensch MR, Jenkins RB (2015) Glioma groups based on 1p/19q, IDH, and TERT promoter mutations in tumors. *N Engl J Med* 372:2499–2508. <https://doi.org/10.1056/NEJMoa1407279>
 32. ElBanan MG, Amer AM, Zinn PO, Colen RR (2015) Imaging genomics of glioblastoma: state of the art bridge between genomics and neuroradiology. *Neuroimaging Clin N Am* 25:141–153. <https://doi.org/10.1016/j.nic.2014.09.010>
 33. Ellingson BM, Bendszus M, Boxerman J, Barboriak D, Erickson BJ, Smits M, Nelson SJ, Gerstner E, Alexander B, Goldmacher G, Wick W, Vogelbaum M, Weller M, Galanis E, Kalpathy-Cramer J, Shankar L, Jacobs P, Pope WB, Yang D, Chung C, Knopp MV, Cha S, van den Bent MJ, Chang S, Yung WK, Cloughesy TF, Wen PY, Gilbert MR, Jumpstarting Brain Tumor Drug Development Coalition Imaging Standardization Steering C (2015) Consensus recommendations for a standardized brain tumor imaging protocol in clinical trials. *Neuro-Oncology* 17:1188–1198. <https://doi.org/10.1093/neuonc/nov095>
 34. Ellingson BM, Cloughesy TF, Pope WB, Zaw TM, Phillips H, Lalezari S, Nghiemphu PL, Ibrahim H, Naeini KM, Harris RJ, Lai A (2012) Anatomic localization of O6-methylguanine DNA methyltransferase (MGMT) promoter methylated and unmethylated tumors: a radiographic study in 358 de novo human glioblastomas. *Neuroimage* 59:908–916. <https://doi.org/10.1016/j.neuroimage.2011.09.076>
 35. Ellingson BM, Lai A, Harris RJ, Selfridge JM, Yong WH, Das K, Pope WB, Nghiemphu PL, Vinters HV, Liau LM, Mischel PS, Cloughesy TF (2013) Probabilistic radiographic atlas of glioblastoma phenotypes. *AJNR Am J Neuroradiol* 34:533–540. <https://doi.org/10.3174/ajnr.A3253>
 36. Fleischmann DF, Unterrainer M, Schon R, Corradini S, Maihofer C, Bartenstein P, Belka C, Albert NL, Niyazi M (2020) Margin reduction in radiotherapy for glioblastoma through (18)F-fluoroethyltyrosine PET? - a recurrence pattern analysis. *Radiother Oncol* 145:49–55. <https://doi.org/10.1016/j.radonc.2019.12.005>
 37. Freyschlag CF, Gruber R, Bauer M, Grams AE, Thome C (2019) Routine postoperative computed tomography is not helpful after elective craniotomy. *World Neurosurg* 122:e1426–e1431. <https://doi.org/10.1016/j.wneu.2018.11.079>
 38. Fujiwara N, Sakatani K, Katayama Y, Murata Y, Hoshino T, Fukaya C, Yamamoto T (2004) Evoked-cerebral blood oxygenation changes in false-negative activations in BOLD contrast functional MRI of patients with brain tumors. *Neuroimage* 21:1464–1471. <https://doi.org/10.1016/j.neuroimage.2003.10.042>
 39. Fureder LM, Widhalm G, Gatterbauer B, Dieckmann K, Hainfellner JA, Bartsch R, Zielinski CC, Preusser M, Berghoff AS (2018) Brain metastases as first manifestation of advanced cancer: exploratory analysis of 459 patients at a tertiary care center. *Clin Exp Metastasis* 35:727–738. <https://doi.org/10.1007/s10585-018-9947-1>
 40. Galldiks N, Dunkl V, Ceccon G, Tscherpel C, Stoffels G, Law I, Henriksen OM, Muhic A, Poulsen HS, Steger J, Bauer EK, Lohmann P, Schmidt M, Shah NJ, Fink GR, Langen KJ (2018) Early treatment response evaluation using FET PET compared to MRI in glioblastoma patients at first progression treated with bevacizumab plus lomustine. *Eur J Nucl Med Mol Imaging* 45:2377–2386. <https://doi.org/10.1007/s00259-018-4082-4>
 41. Galldiks N, Law I, Pope WB, Arbizu J, Langen KJ (2017) The use of amino acid PET and conventional MRI for monitoring of brain tumor therapy. *Neuroimage Clin* 13:386–394. <https://doi.org/10.1016/j.nicl.2016.12.020>
 42. Galldiks N, Stoffels G, Filss C, Rapp M, Blau T, Tscherpel C, Ceccon G, Dunkl V, Weinzierl M, Stoffel M, Sabel M, Fink GR, Shah NJ, Langen KJ (2015) The use of dynamic O-(2-18F-fluoroethyl)-l-tyrosine PET in the diagnosis of patients with progressive and recurrent glioma. *Neuro-Oncology* 17:1293–1300. <https://doi.org/10.1093/neuonc/nov088>
 43. Gempt J, Forschler A, Buchmann N, Pape H, Ryang YM, Krieg SM, Zimmer C, Meyer B, Ringel F (2013) Postoperative ischemic changes following resection of newly diagnosed and recurrent gliomas and their clinical relevance. *J Neurosurg* 118:801–808. <https://doi.org/10.3171/2012.12.JNS12125>
 44. Grand S, Passaro G, Ziegler A, Esteve F, Boujet C, Hoffmann D, Rubin C, Segebarth C, Decors M, Le Bas JF, Remy C (1999) Necrotic tumor versus brain abscess: importance of amino acids detected at 1H MR spectroscopy—initial results. *Radiology* 213:785–793. <https://doi.org/10.1148/radiology.213.3.r99dc10785>
 45. Gregor A, Cull A, Traynor E, Stewart M, Lander F, Love S (1996) Neuropsychometric evaluation of long-term survivors of adult brain tumours: relationship with tumour and treatment parameters. *Radiother Oncol* 41:55–59
 46. Han Y, Yan LF, Wang XB, Sun YZ, Zhang X, Liu ZC, Nan HY, Hu YC, Yang Y, Zhang J, Yu Y, Sun Q, Tian Q, Hu B, Xiao G, Wang W, Cui GB (2018) Structural and advanced imaging in predicting MGMT promoter methylation of primary glioblastoma: a region of interest based analysis. *BMC Cancer* 18:215. <https://doi.org/10.1186/s12885-018-4114-2>
 47. Hartmann M, Heiland S, Harting I, Tronnier VM, Sommer C, Ludwig R, Sartor K (2003) Distinguishing of primary cerebral lymphoma from high-grade glioma with perfusion-weighted

- magnetic resonance imaging. *Neurosci Lett* 338:119–122. [https://doi.org/10.1016/s0304-3940\(02\)01367-8](https://doi.org/10.1016/s0304-3940(02)01367-8)
48. Hegi ME, Diserens AC, Gorlia T, Hamou MF, de Tribolet N, Weller M, Kros JM, Hainfellner JA, Mason W, Mariani L, Bromberg JE, Hau P, Mirimanoff RO, Cairncross JG, Janzer RC, Stupp R (2005) MGMT gene silencing and benefit from temozolomide in glioblastoma. *N Engl J Med* 352:997–1003. <https://doi.org/10.1056/NEJMoa043331>
 49. Hollon T, Stummer W, Orringer D, Suero Molina E (2019) Surgical adjuncts to increase the extent of resection: intraoperative MRI, fluorescence, and Raman histology. *Neurosurg Clin N Am* 30:65–74. <https://doi.org/10.1016/j.nec.2018.08.012>
 50. Hu LS, Ning S, Eschbacher JM, Baxter LC, Gaw N, Ranjbar S, Plasencia J, Dueck AC, Peng S, Smith KA, Nakaji P, Karis JP, Quarles CC, Wu T, Loftus JC, Jenkins RB, Sicotte H, Kollmeyer TM, O'Neill BP, Elmquist W, Hoxworth JM, Frakes D, Sarkaria J, Swanson KR, Tran NL, Li J, Mitchell JR (2017) Radiogenomics to characterize regional genetic heterogeneity in glioblastoma. *Neuro-Oncology* 19:128–137. <https://doi.org/10.1093/neuonc/nw135>
 51. Hutterer M, Nowosielski M, Putzer D, Jansen NL, Seiz M, Schocke M, McCoy M, Gobel G, la Fougere C, Virgolini IJ, Trinka E, Jacobs AH, Stockhammer G (2013) [18F]-fluoro-ethyl-L-tyrosine PET: a valuable diagnostic tool in neuro-oncology, but not all that glitters is glioma. *Neuro-Oncology* 15:341–351. <https://doi.org/10.1093/neuonc/nos300>
 52. Ius T, Isola M, Budai R, Pauletto G, Tomasino B, Fadiga L, Skrap M (2012) Low-grade glioma surgery in eloquent areas: volumetric analysis of extent of resection and its impact on overall survival. A single-institution experience in 190 patients: clinical article. *J Neurosurg* 117:1039–1052. <https://doi.org/10.3171/2012.8.JNS12393>
 53. Jaber M, Wolfer J, Ewelt C, Holling M, Hasselblatt M, Niederstadt T, Zoubi T, Weckesser M, Stummer W (2016) The value of 5-aminolevulinic acid in low-grade gliomas and high-grade gliomas lacking glioblastoma imaging features: an analysis based on fluorescence, magnetic resonance imaging, 18F-fluoroethyl tyrosine positron emission tomography, and tumor molecular factors. *Neurosurgery* 78:401–411; discussion 411. doi:<https://doi.org/10.1227/NEU.000000000001020>
 54. Jakola AS, Berntsen EM, Christensen P, Gulati S, Unsgard G, Kvistad KA, Solheim O (2014) Surgically acquired deficits and diffusion weighted MRI changes after glioma resection—a matched case-control study with blinded neuroradiological assessment. *PLoS One* 9:e101805. <https://doi.org/10.1371/journal.pone.0101805>
 55. Jakola AS, Skjulsvik AJ, Myrmel KS, Sjavik K, Unsgard G, Torp SH, Aaberg K, Berg T, Dai HY, Johnsen K, Kloster R, Solheim O (2017) Surgical resection versus watchful waiting in low-grade gliomas. *Ann Oncol* 28:1942–1948. <https://doi.org/10.1093/annonc/mdx230>
 56. Jansen NL, Schwartz C, Graute V, Eigenbrod S, Lutz J, Egensperger R, Popperl G, Kretschmar HA, Cumming P, Bartenstein P, Tonn JC, Kreth FW, la Fougere C, Thon N (2012) Prediction of oligodendroglial histology and LOH 1p/19q using dynamic [(18)F]FET-PET imaging in intracranial WHO grade II and III gliomas. *Neuro-Oncology* 14:1473–1480. <https://doi.org/10.1093/neuonc/nos259>
 57. Jansen NL, Suchorska B, Wenter V, Eigenbrod S, Schmid-Tannwald C, Zwergal A, Niyazi M, Drexler M, Bartenstein P, Schnell O, Tonn JC, Thon N, Kreth FW, la Fougere C (2014) Dynamic 18F-FET PET in newly diagnosed astrocytic low-grade glioma identifies high-risk patients. *J Nucl Med* 55:198–203. <https://doi.org/10.2967/jnumed.113.122333>
 58. Jenkinson MD, Smith TS, Joyce KA, Fildes D, Broome J, du Plessis DG, Haylock B, Husband DJ, Warnke PC, Walker C (2006) Cerebral blood volume, genotype and chemosensitivity in oligodendroglial tumours. *Neuroradiology* 48:703–713. <https://doi.org/10.1007/s00234-006-0122-z>
 59. Johnson DR, Diehn FE, Giannini C, Jenkins RB, Jenkins SM, Parney IF, Kaufmann TJ (2017) Genetically defined oligodendroglioma is characterized by indistinct tumor borders at MRI. *AJNR Am J Neuroradiol* 38:678–684. <https://doi.org/10.3174/ajnr.A5070>
 60. Kaka N, Hafazalla K, Samawi H, Simpkin A, Perry J, Sahgal A, Das S (2019) Progression-free but no overall survival benefit for adult patients with bevacizumab therapy for the treatment of newly diagnosed glioblastoma: a systematic review and meta-analysis. 11. <https://doi.org/10.3390/cancers11111723>
 61. Kaneko S, Suero Molina E, Ewelt C, Warneke N, Stummer W (2019) Fluorescence-based measurement of real-time kinetics of protoporphyrin IX after 5-aminolevulinic acid administration in human in situ malignant gliomas. *Neurosurgery* 85:E739–E746. <https://doi.org/10.1093/neuros/nyz129>
 62. Kawaguchi T, Sonoda Y, Shibahara I, Saito R, Kanamori M, Kumabe T, Tominaga T (2016) Impact of gross total resection in patients with WHO grade III glioma harboring the IDH 1/2 mutation without the 1p/19q co-deletion. *J Neuro-Oncol* 129:505–514. <https://doi.org/10.1007/s11060-016-2201-2>
 63. Kebir S, Fimmers R, Galldiks N, Schafer N, Mack F, Schaub C, Stuplich M, Niessen M, Tzaridis T, Simon M, Stoffels G, Langen KJ, Scheffler B, Glas M, Herrlinger U (2016) Late pseudoprogression in glioblastoma: diagnostic value of dynamic O-(2-[18F]fluoroethyl)-L-tyrosine PET. *Clin Cancer Res* 22:2190–2196. <https://doi.org/10.1158/1078-0432.CCR-15-1334>
 64. Kebir S, Khurshid Z, Gaertner FC, Essler M, Hattingen E, Fimmers R, Scheffler B, Herrlinger U, Bundschuh RA, Glas M (2017) Unsupervised consensus cluster analysis of [18F]-fluoroethyl-L-tyrosine positron emission tomography identified textural features for the diagnosis of pseudoprogression in high-grade glioma. *Oncotarget* 8:8294–8304. <https://doi.org/10.18632/oncotarget.14166>
 65. Kebir S, Weber M, Lazaridis L, Deuschl C, Schmidt T, Monninghoff C, Keyvani K, Umutlu L, Pierscianek D, Forsting M, Sure U, Stuschke M, Kleinschnitz C, Scheffler B, Colletti PM, Rubello D, Rischpler C, Glas M (2019) Hybrid 11C-MET PET/MRI combined with “machine learning” in glioma diagnosis according to the revised glioma WHO classification 2016. *Clin Nucl Med* 44:214–220. <https://doi.org/10.1097/RLU.0000000000002398>
 66. Keil VC, Pintea B, Gielen GH, Greschus S, Fimmers R, Gieseke J, Simon M, Schild HH, Hadizadeh DR (2017) Biopsy targeting with dynamic contrast-enhanced versus standard neuronavigation MRI in glioma: a prospective double-blinded evaluation of selection benefits. *J Neuro-Oncol* 133:155–163. <https://doi.org/10.1007/s11060-017-2424-x>
 67. Khan MB, Chakraborty S, Boockvar JA (2016) Gross total resection of glioblastoma improves overall survival and progression-free survival compared to subtotal resection or biopsy alone. *Neurosurgery* 79:N12–N13. <https://doi.org/10.1227/01.neu.0000508600.08200.ci>
 68. Kickingereder P, Bonekamp D, Nowosielski M, Kratz A, Sill M, Burth S, Wick A, Eidol O, Schlemmer HP, Radbruch A, Debus J, Herold-Mende C, Unterberg A, Jones D, Pfister S, Wick W, von Deimling A, Bendszus M, Capper D (2016) Radiogenomics of glioblastoma: machine learning-based classification of molecular characteristics by using multiparametric and multiregional MR imaging features. *Radiology* 281:907–918. <https://doi.org/10.1148/radiol.2016161382>
 69. Krings T, Reinges MH, Willmes K, Nuerk HC, Meister IG, Gilsbach JM, Thron A (2002) Factors related to the magnitude of T2* MR signal changes during functional imaging.

- Neuroradiology 44:459–466. <https://doi.org/10.1007/s00234-002-0795-x>
70. Kunz M, Thon N, Eigenbrod S, Hartmann C, Egensperger R, Herms J, Geisler J, la Fougere C, Lutz J, Linn J, Kreth S, von Deimling A, Tonn JC, Kretschmar HA, Popperl G, Kreth FW (2011) Hot spots in dynamic (18)FET-PET delineate malignant tumor parts within suspected WHO grade II gliomas. *Neuro-Oncology* 13:307–316. <https://doi.org/10.1093/neuonc/nuq196>
 71. Lacroix M, Abi-Said D, Fourney DR, Gokaslan ZL, Shi W, DeMonte F, Lang FF, McCutcheon IE, Hassenbusch SJ, Holland E, Hess K, Michael C, Miller D, Sawaya R (2001) A multivariate analysis of 416 patients with glioblastoma multiforme: prognosis, extent of resection, and survival. *J Neurosurg* 95:190–198. <https://doi.org/10.3171/jns.2001.95.2.0190>
 72. Larsen VA, Simonsen HJ, Law I, Larsson HB, Hansen AE (2013) Evaluation of dynamic contrast-enhanced T1-weighted perfusion MRI in the differentiation of tumor recurrence from radiation necrosis. *Neuroradiology* 55:361–369. <https://doi.org/10.1007/s00234-012-1127-4>
 73. Law I, Albert NL, Arbizu J, Boellaard R, Drzezga A, Galldiks N, la Fougere C, Langen KJ, Lopci E, Lowe V, McConathy J, Quick HH, Sattler B, Schuster DM, Tonn JC, Weller M (2019) Joint EANM/EANO/RANO practice guidelines/SNMMI procedure standards for imaging of gliomas using PET with radiolabelled amino acids and [(18)F]FDG: version 1.0. *Eur J Nucl Med Mol Imaging* 46:540–557. <https://doi.org/10.1007/s00259-018-4207-9>
 74. Lawrence YR, Li XA, el Naqa I, Hahn CA, Marks LB, Merchant TE, Dicker AP (2010) Radiation dose-volume effects in the brain. *Int J Radiat Oncol Biol Phys* 76:S20–S27. <https://doi.org/10.1016/j.ijrobp.2009.02.091>
 75. Li YM, Suki D, Hess K, Sawaya R (2016) The influence of maximum safe resection of glioblastoma on survival in 1229 patients: can we do better than gross-total resection? *J Neurosurg* 124:977–988. <https://doi.org/10.3171/2015.5.JNS142087>
 76. Liu X, Mangla R, Tian W, Qiu X, Li D, Walter KA, Ekholm S, Johnson MD (2017) The preliminary radiogenomics association between MR perfusion imaging parameters and genomic biomarkers, and their predictive performance of overall survival in patients with glioblastoma. *J Neuro-Oncol* 135:553–560. <https://doi.org/10.1007/s11060-017-2602-x>
 77. Lohmann P, Werner JM, Shah NJ, Fink GR, Langen KJ, Galldiks N (2019) Combined amino acid positron emission tomography and advanced magnetic resonance imaging in glioma patients. *Cancers (Basil)* 11. <https://doi.org/10.3390/cancers11020153>
 78. Louis DN, Perry A, Reifenberger G, von Deimling A, Figarella-Branger D, Cavenee WK, Ohgaki H, Wiestler OD, Kleihues P, Ellison DW (2016) The 2016 World Health Organization classification of tumors of the central nervous system: a summary. *Acta Neuropathol* 131:803–820. <https://doi.org/10.1007/s00401-016-1545-1>
 79. Matsui Y, Maruyama T, Nitta M, Saito T, Tsuzuki S, Tamura M, Kusuda K, Fukuya Y, Asano H, Kawamata T, Masamune K, Muragaki Y (2020) Prediction of lower-grade glioma molecular subtypes using deep learning. *J Neuro-Oncol* 146:321–327. <https://doi.org/10.1007/s11060-019-03376-9>
 80. Munck Af Rosenschild P, Costa J, Engelholm SA, Lundemann MJ, Law I, Ohlhues L, Engelholm S (2015) Impact of [18F]-fluoro-ethyl-tyrosine PET imaging on target definition for radiation therapy of high-grade glioma. *Neuro-Oncology* 17:757–763. <https://doi.org/10.1093/neuonc/nou316>
 81. Muther M, Koch R, Weckesser M, Sporns P, Schwindt W, Stummer W (2019) 5-Aminolevulinic acid fluorescence-guided resection of 18F-FET-PET positive tumor beyond gadolinium enhancing tumor improves survival in glioblastoma. *Neurosurgery* 85:E1020–E1029. <https://doi.org/10.1093/neuros/nzy199>
 82. Neska-Matuszewska M, Bladowska J, Sasiadek M, Zimny A (2018) Differentiation of glioblastoma multiforme, metastases and primary central nervous system lymphomas using multiparametric perfusion and diffusion MR imaging of a tumor core and a peritumoral zone—searching for a practical approach. *PLoS ONE [Electronic Resource]* 13:e0191341
 83. Nguyen HS, Milbach N, Hurrell SL, Cochran E, Connelly J, Bovi JA, Schultz CJ, Mueller WM, Rand SD, Schmainda KM, LaViolette PS (2016) Progressing bevacizumab-induced diffusion restriction is associated with coagulative necrosis surrounded by viable tumor and decreased overall survival in patients with recurrent glioblastoma. *AJNR Am J Neuroradiol* 37:2201–2208. <https://doi.org/10.3174/ajnr.A4898>
 84. Nicolajilwan M, Hu Y, Yan C, Meerzaman D, Holder CA, Gutman D, Jain R, Colen R, Rubin DL, Zinn PO, Hwang SN, Raghavan P, Hammoud DA, Scarpace LM, Mikkelsen T, Chen J, Gevaert O, Buetow K, Freymann J, Kirby J, Flanders AE, Wintermark M, Group TGPR (2015) Addition of MR imaging features and genetic biomarkers strengthens glioblastoma survival prediction in TCGA patients. *J Neuroradiol* 42:212–221. <https://doi.org/10.1016/j.neurad.2014.02.006>
 85. Nimsky C, Ganslandt O, Cerny S, Hastreiter P, Greiner G, Fahlbusch R (2000) Quantification of, visualization of, and compensation for brain shift using intraoperative magnetic resonance imaging. *Neurosurgery* 47:1070–1079; discussion 1079–1080. doi:<https://doi.org/10.1097/00006123-200011000-00008>
 86. Niyazi M, Brada M, Chalmers AJ, Combs SE, Erridge SC, Fiorentino A, Grosu AL, Lagerwaard FJ, Minniti G, Mirimanoff RO, Ricardi U, Short SC, Weber DC, Belka C (2016) ESTRO-ACROP guideline “target delineation of glioblastomas”. *Radiother Oncol* 118:35–42. <https://doi.org/10.1016/j.radonc.2015.12.003>
 87. Okada H, Weller M, Huang R, Finocchiaro G, Gilbert MR, Wick W, Ellingson BM, Hashimoto N, Pollack IF, Brandes AA, Franceschi E, Herold-Mende C, Nayak L, Panigrahy A, Pope WB, Prins R, Sampson JH, Wen PY, Reardon DA (2015) Immunotherapy response assessment in neuro-oncology: a report of the RANO working group. *Lancet Oncol* 16:e534–e542. [https://doi.org/10.1016/S1470-2045\(15\)00088-1](https://doi.org/10.1016/S1470-2045(15)00088-1)
 88. Oppenlander ME, Wolf AB, Snyder LA, Bina R, Wilson JR, Coons SW, Ashby LS, Brachman D, Nakaji P, Porter RW, Smith KA, Spetzler RF, Sanai N (2014) An extent of resection threshold for recurrent glioblastoma and its risk for neurological morbidity. *J Neurosurg* 120:846–853. <https://doi.org/10.3171/2013.12.JNS13184>
 89. Papp L, Potsch N, Grahovac M, Schmidbauer V, Woehrer A, Preusser M, Mitterhauser M, Kiesel B, Wadsak W, Beyer T, Hacker M, Traub-Weidinger T (2018) Glioma survival prediction with combined analysis of in vivo (11)C-MET PET features, ex vivo features, and patient features by supervised machine learning. *J Nucl Med* 59:892–899. <https://doi.org/10.2967/jnumed.117.202267>
 90. Paulsson AK, McMullen KP, Peiffer AM, Hinson WH, Kearns WT, Johnson AJ, Lesser GJ, Ellis TL, Tatter SB, Debinski W, Shaw EG, Chan MD (2014) Limited margins using modern radiotherapy techniques does not increase marginal failure rate of glioblastoma. *Am J Clin Oncol* 37:177–181. <https://doi.org/10.1097/COC.0b013e318271ae03>
 91. Peeken JC, Goldberg T, Pyka T, Bernhofer M, Wiestler B, Kessel KA, Tafti PD, Nusslin F, Braun AE, Zimmer C, Rost B, Combs SE (2019) Combining multimodal imaging and treatment features improves machine learning-based prognostic assessment in patients with glioblastoma multiforme. *Cancer Med* 8:128–136. <https://doi.org/10.1002/cam4.1908>
 92. Pirotte BJ, Levivier M, Goldman S, Massager N, Wikler D, Dewitte O, Bruneau M, Rorive S, David P, Brotchi J (2009)

- Positron emission tomography-guided volumetric resection of supratentorial high-grade gliomas: a survival analysis in 66 consecutive patients. *Neurosurgery* 64:471–481; discussion 481. <https://doi.org/10.1227/01.NEU.0000338949.94496.85>
93. Pope WB (2018) Brain metastases: neuroimaging. *Handb Clin Neurol* 149:89–112. <https://doi.org/10.1016/B978-0-12-811161-1.00007-4>
 94. Pope WB, Chen JH, Dong J, Carlson MR, Perlina A, Cloughesy TF, Liau LM, Mischel PS, Nghiemphu P, Lai A, Nelson SF (2008) Relationship between gene expression and enhancement in glioblastoma multiforme: exploratory DNA microarray analysis. *Radiology* 249:268–277. <https://doi.org/10.1148/radiol.2491072000>
 95. Price SJ, Young AM, Scotton WJ, Ching J, Mohsen LA, Boonzaier NR, Lupson VC, Griffiths JR, McLean MA, Larkin TJ (2016) Multimodal MRI can identify perfusion and metabolic changes in the invasive margin of glioblastomas. *J Magn Reson Imaging* 43:487–494. <https://doi.org/10.1002/jmri.24996>
 96. Rahman M, Abbatematteo J, De Leo EK, Kubilis PS, Vaziri S, Bova F, Sayour E, Mitchell D, Quinones-Hinojosa A (2017) The effects of new or worsened postoperative neurological deficits on survival of patients with glioblastoma. *J Neurosurg* 127:123–131. <https://doi.org/10.3171/2016.7.JNS16396>
 97. Ricci PE (1999) Imaging of adult brain tumors. *Neuroimaging Clin N Am* 9:651–669
 98. Rios Velazquez E, Meier R, Dunn WD Jr, Alexander B, Wiest R, Bauer S, Gutman DA, Reyes M, Aerts HJ (2015) Fully automatic GBM segmentation in the TCGA-GBM dataset: prognosis and correlation with VASARI features. *Sci Rep* 5:16822. <https://doi.org/10.1038/srep16822>
 99. Rizzo S, Botta F, Raimondi S, Origgi D, Fanciullo C, Morganti AG, Bellomi M (2018) Radiomics: the facts and the challenges of image analysis. *Eur Radiol Exp* 2:36. <https://doi.org/10.1186/s41747-018-0068-z>
 100. Sacko O, Lauwers-Cances V, Brauge D, Sesay M, Brenner A, Roux FE (2011) Awake craniotomy vs surgery under general anesthesia for resection of supratentorial lesions. *Neurosurgery* 68:1192–1198; discussion 1198–1199. doi:<https://doi.org/10.1227/NEU.0b013e31820c02a3>
 101. Sanai N, Polley MY, McDermott MW, Parsa AT, Berger MS (2011) An extent of resection threshold for newly diagnosed glioblastomas. *J Neurosurg* 115:3–8. <https://doi.org/10.3171/2011.2.JNS10998>
 102. Schebesch KM, Proescholdt M, Hohne J, Hohenberger C, Hansen E, Riemenschneider MJ, Ullrich W, Doenitz C, Schlaier J, Lange M, Brawanski A (2013) Sodium fluorescein-guided resection under the YELLOW 560 nm surgical microscope filter in malignant brain tumor surgery—a feasibility study. *Acta Neurochir* 155:693–699. <https://doi.org/10.1007/s00701-013-1643-y>
 103. Schucht P, Beck J, Abu-Isa J, Andereggen L, Murek M, Seidel K, Stieglitz L, Raabe A (2012) Gross total resection rates in contemporary glioblastoma surgery: results of an institutional protocol combining 5-aminolevulinic acid intraoperative fluorescence imaging and brain mapping. *Neurosurgery* 71:927–935; discussion 935–926. doi:<https://doi.org/10.1227/NEU.0b013e31826d1e6b>
 104. Scott JN, Brasher PM, Sevicik RJ, Rewcastle NB, Forsyth PA (2002) How often are nonenhancing supratentorial gliomas malignant? A population study. *Neurology* 59:947–949. <https://doi.org/10.1212/wnl.59.6.947>
 105. Shaver MM, Kohanteb PA, Chiou C, Bardis MD, Chantaduly C, Bota D, Filippi CG, Weinberg B, Grinband J, Chow DS, Chang PD (2019) Optimizing neuro-oncology Imaging: a review of deep learning approaches for glioma imaging. *Cancers (Basel)* 11. <https://doi.org/10.3390/cancers11060829>
 106. Silva MA, See AP, Essayed WI, Golby AJ, Tie Y (2018) Challenges and techniques for presurgical brain mapping with functional MRI. *Neuroimage Clin* 17:794–803. <https://doi.org/10.1016/j.nicl.2017.12.008>
 107. Smith JS, Chang EF, Lamborn KR, Chang SM, Prados MD, Cha S, Tihan T, Vandenberg S, McDermott MW, Berger MS (2008) Role of extent of resection in the long-term outcome of low-grade hemispheric gliomas. *J Clin Oncol* 26:1338–1345. <https://doi.org/10.1200/JCO.2007.13.9337>
 108. Smits M, van den Bent MJ (2017) Imaging correlates of adult glioma genotypes. *Radiology* 284:316–331. <https://doi.org/10.1148/radiol.2017151930>
 109. Sotoudeh H, Shafaat O, Bernstock JD, Brooks MD, Elsayed GA, Chen JA, Szerip P, Chagoya G, Gessler F, Sotoudeh E, Shafaat A, Friedman GK (2019) Artificial intelligence in the management of glioma: era of personalized medicine. *Front Oncol* 9:768. <https://doi.org/10.3389/fonc.2019.00768>
 110. Stockhammer F, Plotkin M, Amthauer H, van Landeghem FK, Woiciechowsky C (2008) Correlation of F-18-fluoro-ethyl-tyrosin uptake with vascular and cell density in non-contrast-enhancing gliomas. *J Neuro-Oncol* 88:205–210. <https://doi.org/10.1007/s11060-008-9551-3>
 111. Stummer W, Meinel T, Ewelt C, Martus P, Jakobs O, Felsberg J, Reifenberger G (2012) Prospective cohort study of radiotherapy with concomitant and adjuvant temozolomide chemotherapy for glioblastoma patients with no or minimal residual enhancing tumor load after surgery. *J Neuro-Oncol* 108:89–97. <https://doi.org/10.1007/s11060-012-0798-3>
 112. Stummer W, Reulen HJ, Meinel T, Pichlmeier U, Schumacher W, Tonn JC, Rohde V, Opperl F, Turowski B, Woiciechowsky C, Franz K, Pietsch T, Group AL-GS (2008) Extent of resection and survival in glioblastoma multiforme: identification of and adjustment for bias. *Neurosurgery* 62:564–576; discussion 564–576. <https://doi.org/10.1227/01.neu.0000317304.31579.17>
 113. Stummer W, Suero Molina E (2017) Fluorescence imaging/agents in tumor resection. *Neurosurg Clin N Am* 28:569–583. <https://doi.org/10.1016/j.nec.2017.05.009>
 114. Stuplich M, Hadizadeh DR, Kuchelmeister K, Scorzin J, Filss C, Langen KJ, Schafer N, Mack F, Schuller H, Simon M, Glas M, Pietsch T, Urbach H, Herrlinger U (2012) Late and prolonged pseudoprogression in glioblastoma after treatment with lomustine and temozolomide. *J Clin Oncol* 30:e180–e183. <https://doi.org/10.1200/JCO.2011.40.9565>
 115. Suchorska B, Giese A, Biczok A, Unterrainer M, Weller M, Drexler M, Bartenstein P, Schuller U, Tonn JC, Albert NL (2018) Identification of time-to-peak on dynamic 18F-FET-PET as a prognostic marker specifically in IDH1/2 mutant diffuse astrocytoma. *Neuro-Oncology* 20:279–288. <https://doi.org/10.1093/neuonc/nox153>
 116. Suchorska B, Jansen NL, Linn J, Kretschmar H, Janssen H, Eigenbrod S, Simon M, Popperl G, Kreth FW, la Fougere C, Weller M, Tonn JC, German Glioma N (2015) Biological tumor volume in 18F-FET-PET before radiochemotherapy correlates with survival in GBM. *Neurology* 84:710–719. <https://doi.org/10.1212/WNL.0000000000001262>
 117. Suero Molina E, Schipmann S, Stummer W (2019) Maximizing safe resections: the roles of 5-aminolevulinic acid and intraoperative MR imaging in glioma surgery—review of the literature. *Neurosurg Rev* 42:197–208. <https://doi.org/10.1007/s10143-017-0907-z>
 118. Suero Molina E, Stummer W (2018) Where and when to cut? Fluorescein guidance for brain stem and spinal cord tumor surgery—technical note. *Oper Neurosurg (Hagerstown)* 15:325–331. <https://doi.org/10.1093/ons/oxp269>
 119. Suero Molina E, Wolfer J, Ewelt C, Ehrhardt A, Brokinkel B, Stummer W (2018) Dual-labeling with 5-aminolevulinic acid and fluorescein for fluorescence-guided resection of high-grade

- gliomas: technical note. *J Neurosurg* 128:399–405. <https://doi.org/10.3171/2016.11.JNS161072>
120. Tan W, Xiong J, Huang W, Wu J, Zhan S, Geng D (2017) Noninvasively detecting Isocitrate dehydrogenase 1 gene status in astrocytoma by dynamic susceptibility contrast MRI. *J Magn Reson Imaging* 45:492–499. <https://doi.org/10.1002/jmri.25358>
 121. Teng J, da Hora CC, Kantar RS, Nakano I, Wakimoto H, Batchelor TT, Chiocca EA, Badr CE, Tannous BA (2017) Dissecting inherent intratumor heterogeneity in patient-derived glioblastoma culture models. *Neuro-Oncology* 19:820–832. <https://doi.org/10.1093/neuonc/now253>
 122. Valentini LG, Casali C, Chatenoud L, Chiaffarino F, Uberti-Foppa C, Broggi G (2008) Surgical site infections after elective neurosurgery: a survey of 1747 patients. *Neurosurgery* 62:88–95; discussion 95–86. doi:<https://doi.org/10.1227/01.NEU.0000311065.95496.C5>
 123. van Dijken BRJ, van Laar PJ, Holtman GA, van der Hooft A (2017) Diagnostic accuracy of magnetic resonance imaging techniques for treatment response evaluation in patients with high-grade glioma, a systematic review and meta-analysis. *Eur Radiol* 27:4129–4144. <https://doi.org/10.1007/s00330-017-4789-9>
 124. Verger A, Stoffels G, Bauer EK, Lohmann P, Blau T, Fink GR, Neumaier B, Shah NJ, Langen KJ, Galldiks N (2018) Static and dynamic (18)F-FET PET for the characterization of gliomas defined by IDH and 1p/19q status. *Eur J Nucl Med Mol Imaging* 45:443–451. <https://doi.org/10.1007/s00259-017-3846-6>
 125. Vettermann F, Suchorska B, Unterrainer M, Nelwan D, Forbrig R, Ruf V, Wenter V, Kreth FW, Herms J, Bartenstein P, Tonn JC, Albert NL (2019) Non-invasive prediction of IDH-wildtype genotype in gliomas using dynamic (18)F-FET PET. *Eur J Nucl Med Mol Imaging* 46:2581–2589. <https://doi.org/10.1007/s00259-019-04477-3>
 126. Voss M, Franz K, Steinbach JP, Fokas E, Forster MT, Filipinski K, Hattingen E, Wagner M, Breuer S (2019) Contrast enhancing spots as a new pattern of late onset pseudoprogression in glioma patients. *J Neuro-Oncol* 142:161–169. <https://doi.org/10.1007/s11060-018-03076-w>
 127. Wakai S, Yamakawa K, Manaka S, Takakura K (1982) Spontaneous intracranial hemorrhage caused by brain tumor: its incidence and clinical significance. *Neurosurgery* 10:437–444. <https://doi.org/10.1227/00006123-198204000-00004>
 128. Wang YY, Wang K, Li SW, Wang JF, Ma J, Jiang T, Dai JP (2015) Patterns of tumor contrast enhancement predict the prognosis of anaplastic Gliomas with IDH1 mutation. *AJNR Am J Neuroradiol* 36:2023–2029. <https://doi.org/10.3174/ajnr.A4407>
 129. Wen PY, Macdonald DR, Reardon DA, Cloughesy TF, Sorensen AG, Galanis E, Degroot J, Wick W, Gilbert MR, Lassman AB, Tsien C, Mikkelsen T, Wong ET, Chamberlain MC, Stupp R, Lamborn KR, Vogelbaum MA, van den Bent MJ, Chang SM (2010) Updated response assessment criteria for high-grade gliomas: response assessment in neuro-oncology working group. *J Clin Oncol* 28:1963–1972. <https://doi.org/10.1200/JCO.2009.26.3541>
 130. White ML, Zhang Y, Kirby P, Ryken TC (2005) Can tumor contrast enhancement be used as a criterion for differentiating tumor grades of oligodendrogliomas? *AJNR Am J Neuroradiol* 26:784–790
 131. Wick W, Chinot OL, Bendszus M, Mason W, Henriksson R, Saran F, Nishikawa R, Revil C, Kerloeguen Y, Cloughesy T (2016) Evaluation of pseudoprogression rates and tumor progression patterns in a phase III trial of bevacizumab plus radiotherapy/temozolomide for newly diagnosed glioblastoma. *Neuro-Oncology* 18:1434–1441. <https://doi.org/10.1093/neuonc/now091>
 132. Wick W, Meisner C, Hentschel B, Platten M, Schilling A, Wiestler B, Sabel MC, Koepfen S, Ketter R, Weiler M, Tabatabai G, von Deimling A, Gramatzki D, Westphal M, Schackert G, Loeffler M, Simon M, Reifenberger G, Weller M (2013) Prognostic or predictive value of MGMT promoter methylation in gliomas depends on IDH1 mutation. *Neurology* 81:1515–1522. <https://doi.org/10.1212/WNL.0b013e3182a95680>
 133. Wijnenga MMJ, French PJ, Dubbink HJ, Dinjens WNM, Atmodimedjo PN, Kros JM, Smits M, Gahrman R, Rutten GJ, Verheul JB, Fleischeuer R, Dirven CMF, Vincent A, van den Bent MJ (2018) The impact of surgery in molecularly defined low-grade glioma: an integrated clinical, radiological, and molecular analysis. *Neuro-Oncology* 20:103–112. <https://doi.org/10.1093/neuonc/nox176>
 134. Willems PW, van der Sprenkel JW, Tulleken CA, Viergever MA, Taphoorn MJ (2006) Neuronavigation and surgery of intracerebral tumours. *J Neurol* 253:1123–1136. <https://doi.org/10.1007/s00415-006-0158-3>

Publisher's note Springer Nature remains neutral with regard to jurisdictional claims in published maps and institutional affiliations.